J. Phys. D: Appl. Phys. **33** (2000) 2791–2797. Printed in the UK PII: S0022-3727(00)14763-1

The after-effect of streamers of positive corona under combined voltage

T Plank, A Haljaste and M Aints

Institute of Experimental Physics and Technology, University of Tartu, 51010 Tartu, Estonia

Received 16 June 2000

Abstract. The rise probabilities of positive corona streamers initiated by a flux of negative ions are investigated under the combined voltage (dc + ac) in point-to-coaxial cylinder discharge gaps in atmospheric air. A method is developed to detect and to estimate quantitatively an after-effect of the preceding streamer on the rise probability of the following one during the next cycle of the ac voltage. The method is based on the statistical analysis of sequences of streamers. The dependence of the intensity of the after-effect on dc and ac voltage, ac frequency, pre-ionization level, air humidity and airflow velocity is investigated. The causes of the after-effect of streamers are discussed.

1. Introduction

In our previous works, we have investigated physical phenomena in a streamer counter [1, 2]. The streamer counter is a corona-based device where the dependence of the repetition rate of corona streamers on the concentration of electronegative additives is used for the detection of electronegative trace gases in air [3]. Under some experimental conditions in the streamer counter, the preceding streamer changed the rise probability of the following one [1]. This after-effect of streamers complicated both the detector calibration and the interpretation of the readings.

In air, the after-effect of a discharge on the rise and development of the next discharge is usually attributed to residual ions [4, 5], chemical products (ozone, nitrous oxides, etc) [6, 7] and neutral excited species [5]. Detachment of electrons from negative ions under the influence of the applied electric field is the dominant creation process of free electrons for triggering a corona discharge [4, 5, 8–13]. The changes in rise probability of a discharge are caused mainly by the residual negative ions. They come from a discharge channel; they may be produced by a previous corona pulse due to the photoeffect at the surface of the opposite electrode or due to the photoionization of gas molecules.

Although different manifestations of the after-effect of corona pulses are widely investigated, special methods for their detection are poorly developed. Very few attempts have been made with the aim of quantifying these phenomena under controlled conditions.

This paper deals with the after-effect of a streamer upon the rise of the streamer during the next cycle of the combined (dc + ac) voltage. The main objective of this investigation was to develop a method suitable for the detection of the after-effect of streamers and quantitative estimation of its intensity. The after-effect was investigated depending on dc and ac voltage, ac frequency, airflow rate, pre-ionization level, humidity of the air, and geometry of the discharge gap. In order to clarify the physical background of the after-effect in a streamer counter, we simulated numerically the ion trajectories in the discharge gaps and measured the length of streamers. Finally, the flux of negative ions created by the previous streamer and responsible for the after-effect was calculated numerically under the assumption that ions were formed only due to the photoionization. The experimental and computed results were compared.

2. Detection of an after-effect of streamers under combined voltage: theoretical background of the method

A better understanding of the proposed method requires a brief description of some features characteristic to the discharge mechanism in a streamer counter under the combined voltage. Here, we use some oscillograms (figure 1) recorded in our experimental device (see section 3 for more information). In figure 1, the upper oscillogram represents the combined voltage, which is applied to the point electrode. Here U_{bp} denotes the onset voltage of burst pulses, U_{str} that of streamers, and U_g that of steady glow corona. Δt_{bp} is the time interval during which the resultant voltage increases from U_{bp} to U_{str}. Negative ions, created by an ionizer and carried by the air stream and by the electric field to the discharge gap, are the source of triggering electrons. Free electrons for triggering a corona discharge appear via collisional detachment from negative ions under the influence of the strong electric field near the point electrode. Due to the stochastic nature of the appearance of triggering electrons the discharge arises during each cycle either as a burst pulse or a streamer [1].

0022-3727/00/212791+07$30.00

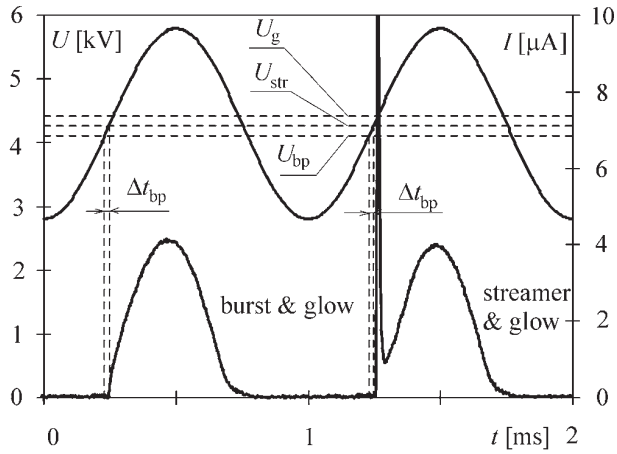

Figure 1. Typical oscillograms of applied voltage and discharge current: point diameter $d = 0.5$ mm.

A certain probability exists for the rise of a burst pulse, if an electron appears in the active zone during Δt_{bp}. The burst pulse spreads over the hemispherical tip of the point. The positive space charge of the burst pulse blocks the rise of a streamer [14, 15] for a time sufficient for the increasing voltage to reach the onset voltage of the steady glow corona, U_g. Thus, the burst pulse is transformed smoothly into the steady glow corona and no streamer is able to develop at this ac cycle. In figure 1, the first pulse in the current oscillogram corresponds to that situation.

If an appropriately placed triggering electron does not appear during Δt_{bp}, then such a later electron initiates a streamer during that ac half-cycle [1]. In figure 1, the second current pulse illustrates this case. Under the conditions of our experiments, only a single streamer arises during one ac cycle. The streamers are followed by the glow corona. The intensity of the glow corona is approximately the same, both after a burst pulse and after a streamer. The steady glow corona burns on the point electrode as long as the resultant voltage, U, is above U_{bp}. When the resultant voltage sinks below U_{bp}, the corona interrupts.

If the rise of a burst pulse during the time interval Δt_{bp} excludes the rise of a streamer during this ac cycle, then the rise probability, P , of a streamer is given by the formula [1]

$$P = \exp\left(-\Phi_T b \Delta t_{bp}\right). \tag{1}$$

Here Φ_T is a stochastic flux of negative ions reaching this part of the active zone ahead of the point electrode where a detached electron can initiate a burst pulse. Below this region of the active zone at $U = U_{str}$ will be referred to as the birth region of burst pulses. The calculation of the lateral boundary of this region will be discussed in section 4.

In expression (1), b denotes the mean (averaged over the voltage interval $U_{bp} \leqslant U \leqslant U_{str}$ and over the birth region of burst pulses) probability of initiation of a burst pulse by a single negative ion. The value of b depends on the diameter of the point electrode [16] and the nature of ions. Expression (1) is valid, if the pre-ionization level is high enough to ensure the discharge inception at each ac cycle. In practice, we get the rise probability of a streamer, P, by dividing the total number of streamers by the total number of the consecutive ac cycles examined.

Let us suppose now that some negative ions left in the discharge gap by a streamer and glow corona are available during the next increase in the combined voltage so that they form a supplementary ion flux into the birth region of burst pulses in addition to the flux from the ionizer. This supplementary ion flux increases the rise probability of a burst pulse and decreases the rise probability of a streamer. The intensity of the supplementary ion flux caused by a streamer and a following glow is evidently different from the flux caused solely by the glow corona. From the above, we conclude that the rise probability of a discharge during the given ac cycle may depend on the type of the discharge of the preceding ac cycle. For the detection of such an after-effect of a discharge, we introduce two more rise probabilities of a streamer, P_{as} and P_{ab}, as follows.

(1) P_{as} denotes the rise probability of a streamer for an ac cycle that is preceded by the ac cycle with a streamer.
(2) P_{ab} denotes the rise probability of a streamer for an ac cycle that is preceded by the ac cycle without any streamer; that is, during the foregoing cycle the discharge has been started as a burst pulse which is followed by the glow corona without any streamers.

For the calculation of P_{as} and P_{ab}, a sequence of streamers must be recorded synchronously with the ac voltage. The set of recorded ac cycles should be split up into two subsets. The first subset includes all these ac cycles that are preceded by the cycle with a streamer and glow. The second one includes all remaining ac cycles; that is, the cycles which are preceded by the cycle with a burst pulse and glow without any streamers. Dividing the number of streamers in the first subset by the number of ac cycles in this subset, we get P_{as} (probability after streamer). In the second subset, the analogous procedure gives P_{ab} (probability after burst pulse). Probabilities P, P_{as} and P_{ab} are related according to the formula

$$P = \frac{P_{ab}}{1 - (P_{as} - P_{ab})}.$$

The total flux, Φ_T, of negative ions into the birth region of burst pulses may consist of up to three components, if the after-effect of a previous discharge exists. The first component, Φ_0, is due to the external ionizer. The second component, Φ_s, is due to the residual ions of the preceding streamer. The third component, Φ_g, is caused by the residual ions left in the gap by the preceding glow corona. As a first approximation, we suppose that the ions of each flux component have the same age, whereas the ions of different flux components have different ages. The probability of initiation of a burst pulse by a single negative ion may therefore be different for the different components of the ion flux. Let b_0, b_s and b_g denote these (mean) probabilities for the ions in the corresponding flux components Φ_0, Φ_s and Φ_g, respectively. Now formula (1) can be rewritten for P_{as} and P_{ab} as follows:

$$P_{as} = \exp\left\lfloor -\left(\Phi_0 b_0 + \Phi_g b_g + \Phi_s b_s\right) \Delta t_{bp} \right\rfloor \tag{2}$$

$$P_{ab} = \exp\left\lfloor -\left(\Phi_0 b_0 + \Phi_g b_g\right) \Delta t_{bp} \right\rfloor. \tag{3}$$

The intensity of the glow corona is approximately the same, both after a burst pulse and after a streamer (see figure 1).

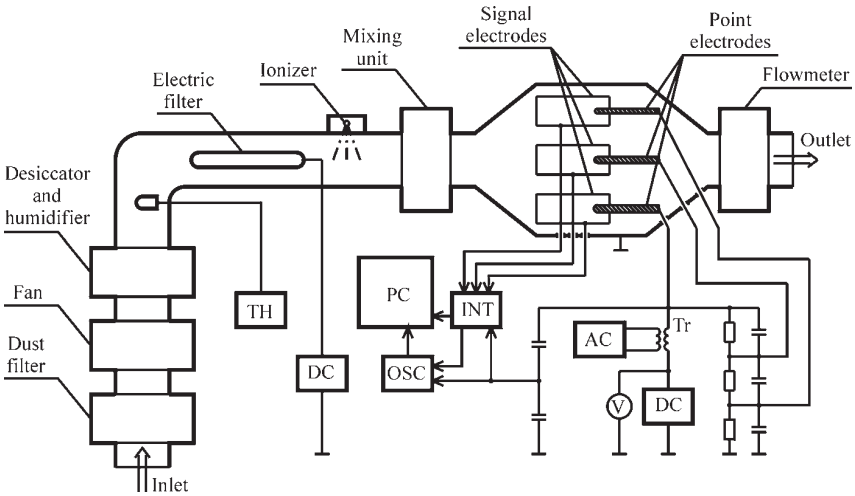

Figure 2. Experimental set-up.

The after-effect of the glow corona, if it exists, should be present therefore during each ac cycle in equal measure, independent of streamers. Regarding this, it follows from formulae (2) and (3):

$$\Phi_s b_s = \frac{1}{\Delta t_{bp}} \ln\left(\frac{P_{ab}}{P_{as}}\right). \tag{4}$$

The product $\Phi_s b_s$ can be considered as a quantitative measure of the after-effect of a streamer, because it represents the effective supplementary ion flux during the time interval Δt_{bp}.

Only few words have been said above about the role of the residual positive ions. In specific cases, the positive space charge of a decaying streamer channel can affect the rise probability of the next streamer because the field conditions may be changed. Under our conditions, the positive space charge ahead of the point electrode is predominantly removed long before the rise of the next discharge due to drift and diffuse scattering of the charges, and the negative ions play the major role in the after-effect studied. In principle, an effect of the positive ions may appear at high ac frequencies.

3. Experimental set-up

We investigated the after-effect of discharge pulses in an electrode arrangement designed for a streamer counter. Figure 2 shows a diagram of the experimental set-up. Hemispherically tipped platinum wires of different diameter, d, ($d = 0.13$, 0.25 and 0.50 mm) served as point electrodes. Each of these was surrounded by a coaxial cylinder as an opposite electrode of 28 mm in inner diameter and 30 mm in length. The point tip was placed 25 mm distant from the front edge of the cylinder. The cylinders served as signal electrodes. In the following, these discharge gaps of the multielectrode streamer counter will be called channel 1, channel 2 and channel 3, respectively. High dc and ac voltages, U_{dc} and U_{ac}, were applied to the point electrodes through a common rc voltage divider. Frequency of the ac voltage, f, was varied from 200–1100 Hz. Circuit arms of the voltage divider were chosen so that the combined voltage reached the onset voltage of streamers for all gaps simultaneously. The dc voltage was adjusted close to the onset voltage of streamers. The onset voltages of different discharge modes are presented in table 1.

Table 1. Onset voltages.

Point diameter, d (mm)	0.13	0.25	0.50
U_{bp} (kV)	2.46	3.08	4.10
U_{str} (kV)	2.54	3.18	4.26
U_g (kV)	2.84	3.43	4.42

A digital dual-channel 60 MHz oscilloscope recorded the pulses induced on the signal electrodes. A personal computer, PC, with a special interface, INT, stored both the sequences of streamers and the ac voltage synchronously. The time resolution and the recording time were 1 μs and 5 s, respectively.

A dust filter eliminated particles larger than 10 nm in diameter from the laboratory air. A desiccator filled with silica gel removed moisture from the air. The desired level of humidity was adjusted thereafter by evaporation of distilled water in a humidification unit. A digital thermohygrometer, TH, measured the humidity and air temperature. The experiments were carried out at a pressure of 1.01×10^5 Pa, at a temperature of 20 °C and at an absolute humidity $\rho = 3.1$ g m^{-3}. The volumetric flow rate of the gas stream was measured by a differential flowmeter.

An electric filter neutralized primary air ions. A subsequent α-active ionizer generated free electrons and ions in the air. Under normal air conditions, the free electrons have a characteristic attachment lifetime of $\sim 10^{-8}$ s [17]. They attach to electronegative atoms and molecules in the zero field near the ionizer. A homogeneous mixture of ions was obtained in a mixing unit. The ion flux, Φ, at the inlet of the signal electrodes was measured with an electrometer in additional experiments. Below, while discussing the pre-ionization level, we consider just this ion flux. The age of ions in the flux, Φ, was approximately 0.3 s. During the experiments, the pre-ionization level was always such that the increase in pre-ionization decreased the rise probability of streamers. At the same time, the pre-ionization level was too low for changing the discharge mechanism.

4. Computer modelling of ion flow

The aim of the computer modelling was to discover whether the residual negative ions responsible for the after-effect come from a discharge channel; whether they are produced due to the photoeffect at the surface of the opposite electrode or due to the photoionization of gas molecules.

In numerical two-dimensional calculations, we evaluated the motion of ions as a resultant drift caused by both the air flux and the electric field. The distribution of the axisymmetric Laplacian electric field, $E(r, z)$, in the cylindrical coordinates was computed by the finite difference method using the Gauss–Seidel iterative condition [18]. The rectangular computation area was divided into a square grid having maximally 3200 nodes per millimetre. It was taken for the convergence criterion of the iterations that the relative residual in the iterative process must be less than 10^{-12} at each interior node.

The air flux was taken into account as an additional electric field $\vec{E}_{\text{flow}}(r) = \vec{v}(r)/\mu$, where $\vec{v}(r)$ was the vector of the airflow velocity, r was a radial coordinate, and μ was the mobility of ions. Computations were carried out on the assumption that the mobility of negative ions, μ, was 2 cm^2 (Vs)$^{-1}$. The airflow profile inside the signal electrode was calculated according to the empirical power-law equation $v(r) = v(0)(1 - r/R_0)^{1/1.66\log(Re)}$, where R_0 was the coordinate of the wall of the signal electrode and Re was the Reynolds number [19]. In our experiments and calculations, Re ranged from 1240–5500.

At the onset of burst pulses only these avalanches, which develop close to the axis of the discharge gap, can launch the burst pulses [14]. We consider the size (number of electrons) of those avalanches to be critical and calculate it using the numerically computed Laplacian field, and the data for the ionization coefficient from the survey [20]. Our estimate of the size of the critical avalanche is, depending on the point diameter, $(1.1 - 2.9) \times 10^4$ electrons. The size of the critical avalanche is larger for fine point electrodes.

Once the onset voltage of burst pulses is exceeded, it is possible for the electrons in the off-axis positions to launch burst pulses. The upper voltage limit for burst pulses is U_{str}. The utmost off-axis start position of a critical avalanche at $U = U_{\text{str}}$ determines the lateral boundary of the birth region of burst pulses. The computed ratio of the distance of that lateral boundary from the gap axis and the radius of the point electrode is approximately 0.68 for all three channels.

Figure 3 presents for channel 3 ($d = 0.50$ mm) the ion trajectories terminating at the lateral boundary of the birth region of burst pulses in the case of different velocities, v, of the airflow. These ion trajectories, later called limiting trajectories, are computed and displayed inside the signal electrode in the plane of the gap axis. Similar calculations for finer point electrodes reveal that the smaller the diameter of the point electrode is, the closer the limiting trajectories are to the gap axis.

We determined numerically the coordinates of the space region inside which the negative ions were collected on the point electrode during the time interval $1/f - \Delta t_{\text{bp}}$. The sectional view of this space region in the plane of the gap axis for $v = 0.8$ m s^{-1} is painted grey in figure 3. The gap

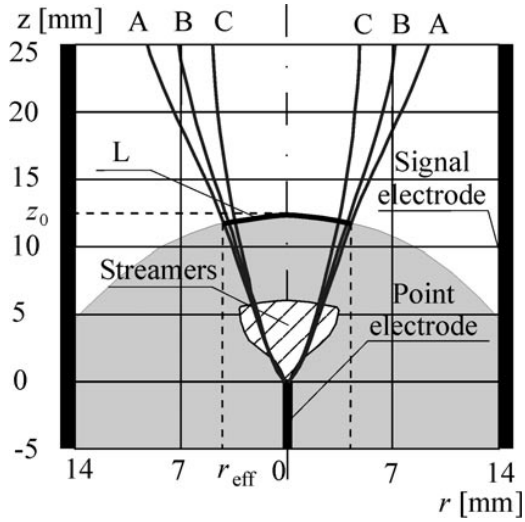

Figure 3. Trajectories of ions, terminating at the lateral boundary of the birth region of burst pulses: $d = 0.5$ mm; $f = 1000$ Hz; $U_{\text{dc}} = 4.40$ kV; $U_{\text{ac}} = 1500$ V. (A) $v = 0.8$ m s^{-1}; (B) $v = 1.4$ m s^{-1}; (C) $v = 3.2$ m s^{-1}.

axis intersects the boundary of this space region at $z = z_0$. The value of z_0 increases with a decrease in the ac frequency and with an increase in the airflow rate or dc voltage. An ion layer, labelled L in figure 3, is located between the limiting trajectories immediately beyond that boundary. The ions of this layer are responsible for the initiation of the discharge one ac period later, during the time interval Δt_{bp}. The radial extent of the layer, L, we denote with r_{eff}. The thickness of the layer is equal to $v_{\text{i}}\Delta t_{\text{bp}}$, where $\vec{v}_{\text{i}} = \vec{v} + \mu\vec{E}$ is the velocity of ions in the layer, L. The region occupied by streamer channels is indicated in the same figure. The length of streamers, l, was measured visually and photographically using a signal electrode with a hole for visual observations. The lengths of streamers were 2.4, 3.6 and 5.9 mm for point diameters $d = 0.13$ mm, $d = 0.25$ mm and $d = 0.50$ mm, respectively.

5. Results and discussion

Figure 4 shows that in channel 1 the probabilities P_{as} and P_{ab} coincide within the limits of experimental accuracy over all the dc voltage range except the beginning of the curves. In channel 2, the initially different probabilities become equal at $U_{\text{dc}} > 3.6$ kV. In channel 3, the probabilities differ markedly over the whole range of the dc voltage. The difference between P_{as} and P_{ab} indicates that the after-effect of a streamer exists.

Calculation of ion trajectories enables us to clarify the background of the negative ions responsible for the after-effect. The negative ions can arise due to the photoeffect on the wall of the signal electrode and the subsequent attachment of photoelectrons to the oxygen molecules near the wall. If the airflow is laminar and $v > 0.8$ m s^{-1}, then in all three channels these ions are unable to reach the birth region of burst pulses (see figure 3) and to participate in the initiation of the discharge.

In figure 3, we can see that the streamer length is at least two times less than z_0. Hence, the ions born in the steamer channel should be removed before the rise of the

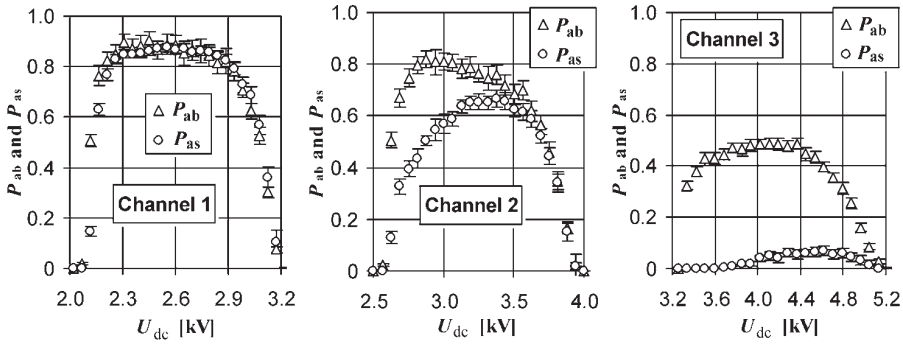

Figure 4. Rise probabilities of streamers depending on the dc voltage: $f = 1000$ Hz; $v = 1.4$ m s^{-1}; $\Phi = 3.04 \times 10^5$ s^{-1}. Channel 1, $U_{ac} = 430$ V; channel 2, $U_{ac} = 570$ V; channel 3, $U_{ac} = 890$ V.

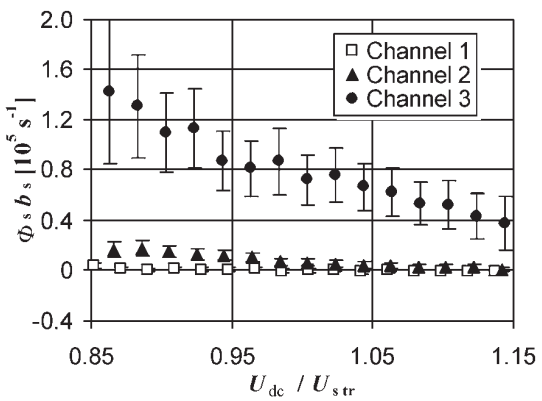

Figure 5. The product $\Phi_s b_s$ depending on the reduced dc voltage: $f = 1000$ Hz; $v = 1.4$ m s^{-1}; $\Phi = 3.04 \times 10^5$ s^{-1}. Channel 1, $U_{ac} = 430$ V; channel 2, $U_{ac} = 570$ V; channel 3, $U_{ac} = 890$ V.

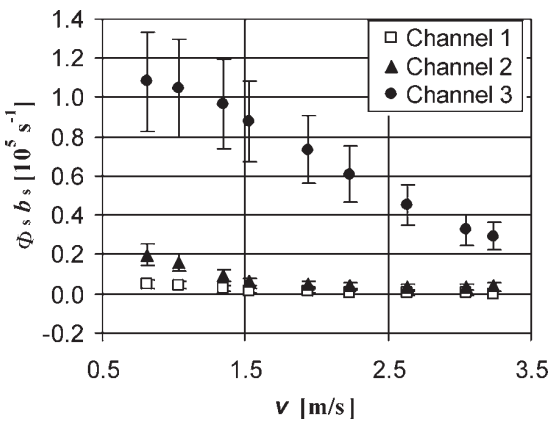

Figure 6. The product $\Phi_s b_s$ depending on the airflow velocity: $f = 1000$ Hz; $\Phi = 1.97 \times 10^5$ s^{-1}–4.54×10^5 s^{-1}. Channel 1, $U_{dc} = 2.41$ kV; $U_{ac} = 740$ V; channel 2, $U_{dc} = 3.13$ kV and $U_{ac} = 980$ V; channel 3, $U_{dc} = 4.27$ kV and $U_{ac} = 1520$ V.

next discharge and therefore they are unable to contribute to the after-effect.

The negative ions may be produced due to an ionizing radiation [14, 21, 22] of the previous streamer, which produces the electron–ion pairs also in the layer, L. Fast attachment of photoelectrons results in the formation of negative ions that are responsible for the after-effect because they reach the birth region of burst pulses one ac period later, during the time interval Δt_{bp}.

Figure 5 displays a quantitative characteristic of the after-effect, the effective ion flux, $\Phi_s b_s$, depending on the applied dc voltage, U_{dc}, reduced to the onset voltage of streamers in the corresponding channel. This flux is calculated according to formula (4). Under the combined voltage, the mean charge of streamers remains nearly unchanged by the dc voltage, because most streamers arise only slightly above the onset voltage, U_{str}. An increase in dc voltage causes an increase in z_0. Therefore, the number density of photoions decreases in the layer, L, and the after-effect of a streamer weakens.

Figure 6 demonstrates how the after-effect of the previous streamer depends on the airflow velocity, v. An increase in the airflow rate causes a more effective removal of the discharge products and a corresponding weakening of the after-effect of a streamer.

Figure 7 presents $\Phi_s b_s$ as a function of the frequency

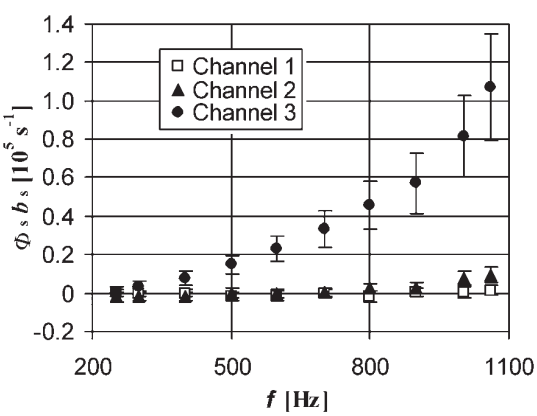

Figure 7. The product $\Phi_s b_s$ depending on the frequency of the ac voltage: $v = 1.4$ m s^{-1}; $\Phi = 3.04 \times 10^5$ s^{-1}. Channel 1, $U_{dc} = 2.41$ kV and $U_{ac} = 720$ V; channel 2, $U_{dc} = 3.13$ kV and $U_{ac} = 950$ V; channel 3, $U_{dc} = 4.28$ kV and $U_{ac} = 1490$ V.

of the ac voltage. The time interval between discharges of subsequent ac cycles shortens with an increase in the frequency of the ac voltage. Consequently, less time is available for the removal of residual products. z_0 decreases and the number density of photoions in the layer, L, increases. As a result, the after-effect of a streamer enhances.

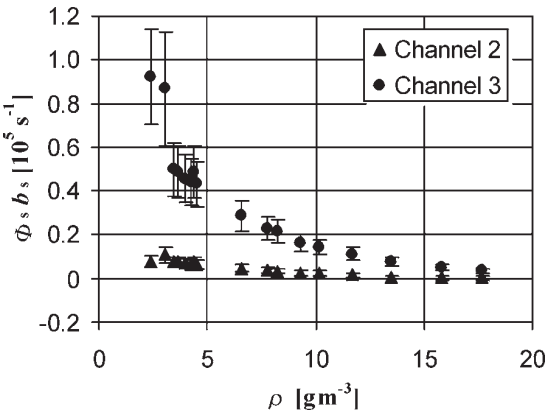

Figure 8. The product $\Phi_s b_s$ depending on the air humidity: $f = 1000$ Hz; $\Phi = 3.04 \times 10^5$ s^{-1}; $v = 1.4$ m s^{-1}. Channel 2, $U_{dc} = 3.07$ kV and $U_{ac} = 600$ V; channel 3, $U_{dc} = 4.19$ kV and $U_{ac} = 930$ V.

The effective flux of residual negative ions must be independent of the pre-ionization level maintained by the ionizer. Hence, an increase in the pre-ionization level reduces the relative contribution of the residual ions. The experiments confirm these considerations.

In our experiments where $U_{dc} \approx U_{str}$, the changes in peak value of the ac voltage, U_{ac}, had no influence on the intensity of the after-effect of a streamer.

Figure 8 demonstrates that the after-effect of a streamer weakens with an increase in the concentration of water vapour. Due to the water vapour in the air, absorption of the photoionizing radiation increases [14]. As a result, the number density of photoions increases near the streamer channel and decreases in the layer, L. The water vapour causes also a marked decrease in the length and the charge of a streamer [14], which in its turn reduces the number density of photoions. Moreover, in the moist air, the electron detachment from complex ions is less probable. The probability, b_s, of initiation of a burst pulse by a residual complex photoion decreases. As a result, the after-effect of a streamer will decrease in the moist air.

Considering figures 5–8 one can see that the after-effect of a streamer weakens with a decrease in the point diameter. This happens mainly because the volume of the layer, L, decreases. The average length and power of a streamer also decrease with the point diameter. Both processes decrease the number of photoions in the layer, L, and the after-effect of a streamer weakens.

We calculated numerically the flux of ions, Φ_s, as if the ions were generated by the radiation of a streamer only, using the photoionization data obtained by Teich [21]. Teich measured the total number of ion pairs, Ψ, produced by photoionization in a 1 cm thick spherical layer (in the solid angle of 4π sr) at various distances from an avalanche per unit pressure and per one ionizing collision in the avalanche. In our case, the photoions responsible for the after-effect were generated by a streamer in a layer, L, located at a distance, z_0, from the point electrode. We had to take into account the fact that the streamer was a bulk source of radiation. As a simplification, we considered a streamer to be an unbranched single discharge channel developing instantaneously along

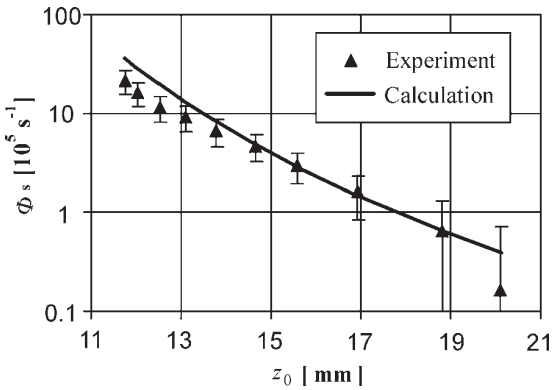

Figure 9. Flux of photoions, Φ_s, depending on z_0.

the gap axis up to the length, l. The local number of ionizing collisions in a channel element of length, dz, is proportional to the number of electrons there. The number of electrons in a discharge was found to be proportional to the intensity of the emitted light, I [23]. The distribution of the light intensity of a branched streamer, $I(z)$, along the gap axis was measured experimentally [24]. Knowing from the current measurements the total charge, Q, of the streamer, we calculate the unknown local number of ionizing collisions as

$$Q\left[e\int_0^l I(z)\,\mathrm{d}z\right]^{-1} I(z)\,\mathrm{d}z.$$

Here e denotes the elementary charge. For the ion flux, Φ_s, we write the integral in the form:

$$\Phi_s(z_0) \approx \frac{Qpv_i(0,z_0)}{4\pi e\int_0^l I(z)\,\mathrm{d}z}\int_0^l \left[I(z)\Theta(z)\Psi(pz_0-pz)\right]\mathrm{d}z \tag{5}$$

where p is the pressure and $\Theta(z)$ is the solid angle under which the layer, L, is visible from an element of the streamer channel located at point z. Formula (5) is an approximate one because, in addition to the simplifications mentioned above, we disregard the real geometry of the layer, L, and the real distribution of ion mobilities.

Calculating Φ_s for different ac frequencies, we plot Φ_s as a function of the axial coordinate, z_0, of the layer, L. The line in figure 9 presents the calculated flux in channel 3. Measured flux is given by dots. All parameters are those indicated for figure 7. The value of the rise probability, b_s, needed for the calculation of Φ_s from $\Phi_s b_s$, we estimated (under the assumption that $b_s \approx b_0$) according to the algorithm proposed in paper [16]. In channel 3 ($d = 0.5$ mm) $b_s \approx 0.047$ for the ions of 0.3 s age.

The measured and calculated fluxes are in close agreement. On the one hand, this result demonstrates that the investigated after-effect of a streamer is originated by photoionization. On the other hand, it confirms that the method proposed in this paper is suitable for quantitative evaluation of the after-effect.

6. Conclusions

A method is developed to investigate the after-effect of a streamer on the rise of the following streamer. The method is based on the statistical analysis of sequences of streamers under the condition of the combined voltage (dc + ac). The negative ions left in the discharge gap by the previous streamer cause the after-effect. The method enables us to measure the flux of these ions. The analysis of the experimental results, as well as the two-dimensional numerical simulation of the ion drift in the air flux, reveal that the negative ions responsible for the after-effect are the products of photoionization. As the investigated device (streamer counter) is capable of operating as a detector of electronegative trace gases, the present results give a better understanding of the features peculiar to that device. The proposed detection method of the after-effect of streamers enables us, in each specific case, to select preferable parameters of the streamer counter so that the absence of the after-effect will be guaranteed.

Acknowledgment

The Estonian Science Foundations supported this work financially under Grant 3024.

References

[1] Aints M, Haljaste A, Kudu K and Plank T 1997 Repetition rate of streamers as a measure of content of electronegative additives in the air *J. Phys. D: Appl. Phys.* **30** 210–20

[2] Aints M, Haljaste A, Kudu K and Plank T 1996 Dependence of streamer corona characteristics on the concentration of electronegative trace gases in air *Proc. 5th Int. Symp. on High Pressure Low Temperature Plasma Chem. (Milovy)* pp 117–21

[3] Kudu K 1980 Some possible applications of a streamer counter *Proc. 6th Int. Conf. on Gas Discharges and Applications* Part 1 (Edinburgh: Heriot-Watt University Press) pp 275–8

[4] Waters R T 1978 *Spark Breakdown in Non-uniform Fields Electrical Breakdown of Gases* ed J M Meek and J D Craggs (Chichester: Wiley) pp 385–532

[5] Goldman M and Goldman A 1978 *Corona Discharges Gaseous Electronics. Electrical Discharges* vol 1, ed M N Hirsh and H J Oskam

[6] Gosho Y 1981 Enhancement of dc positive streamer corona in a point-plane gap in air due to addition of a small amount of an electronegative gas *J. Phys. D: Appl. Phys.* **14** 2035–46

[7] Gosho Y 1982 Considerable change in dc breakdown characteristics of positive-point–plane gaps due to varying concentrations of NO_X, CO_2 and H_2O in air and intensity of irradiation *J. Phys. D: Appl. Phys.* **15** 1217–25

[8] Andersson N E 1958 An investigation of the positive point streamer corona. Part I. The time distribution of the streamers *Arkiv Fysik* **13** 399–422

[9] Waters R T, Jones R E and Bulcock C J 1965 Influence of atmospheric ions on impulse corona discharge *Proc. IEE* **112** 1431–8

[10] Hepworth J K, Klewe R C and Tozer B A 1972 The effect of charged particles on impulse corona and breakdown in divergent field gaps *Proc. Int. Conf. Gas Discharges (London)* pp 227–9

[11] Gallimberti I 1979 The mechanism of the long spark formation *J. Physique* **40** C7 193–250

[12] Gosho Y and Harada A 1982 A new technique for detecting initial electrons by using Geiger counter region of positive corona *Proc. 7th Int. Conf. on Gas Discharges and Applications (London)* pp 193–5

[13] Gosho Y and Saeki M 1987 Triggering of dc positive corona by pulsed UV irradiation *J. Phys. D: Appl. Phys.* **20** 526–9

[14] Loeb L B 1965 *Electrical Coronas: Their Basic Physical Mechanisms* (Berkeley and Los Angeles: University of California Press)

[15] Miyoshi Y and Hosokawa T 1973 The formation of a positive corona in air *J. Phys. D: Appl. Phys.* **6** 730–3

[16] Plank T, Aints M and Haljaste A 1999 Investigation of rise probability of positive corona initiated by negative ions *Proc 24th Int. Conf. on Phenomena in Ionized Gases (Warsaw)* vol II, pp 145–6

[17] Bazelyan E M and Raizer J P 1998 *Spark Discharge* (Boca Raton, FL: CRC Press)

[18] Zhou P 1993 *Numerical Analysis of Electromagnetic Fields* (Berlin: Springer)

[19] Miller R W 1989 *Flow Measurement Engineering Handbook* 2nd edn (New York: McGraw-Hill)

[20] Dutton J A 1975 Survey of electron swarm data *J. Phys. Chem. Ref. Data* **4** 577-–856

[21] Teich T H 1967 Emission gasionisierender Strahlung aus Elektronlawinen *Z. Phys.* **199** 378–410

[22] Penney G W and Hummert G T 1970 Photoionization measurements in air, oxygen, and nitrogen *J. Appl. Phys.* **41** 572–7

[23] Raether H 1964 *Electron Avalanches and Breakdown in Gases* (London: Butterworths)

[24] Korge H, Kudu K and Laan M 1977 Development of dc corona pulses at atmospheric pressure *Proc 13th Int. Conf. on Phenomena in Ionized Gases (Berlin)* pp 451–2